

<https://doi.org/10.30678/ft.88768>

© 2020 The Authors

Open access (CC BY 4.0)

Analytical Study of Non-Recessed Conical Hole Entry Hybrid/Hydrostatic Journal Bearing with Constant Flow Valve Restrictor

Prashant G. Khakse¹, Vikas M. Phalle²¹Senior Engineer, Engineering Maintenance Training Organization, Air India Engineering Services limited, Mumbai 400029, India.²Associate Professor, Laboratory of Machine Dynamics and Vibration, Department of Mechanical Engineering, VJTI, Mumbai 400019, India.

Corresponding author: Prashant G. Khakse (prashantkhakse@yahoo.com)

ABSTRACT

The present work studies the analysis of a non recessed hole entry conical hybrid/hydrostatic journal bearing adjusted for constant flow valve (CFV) restriction. The paper provides effectiveness between the conical bearings with hole entry operating in hybrid and hydrostatic mode. The Reynolds formulae, for the flow of fluid through the mating surfaces of a conical journal and bearing, are numerically worked out in both the modes considering the finite element analysis (FEA) and the necessary boundary preconditions. Holes in double row are marked on conical bearing circumference to accommodate the CFV restrictors, the angular distance between two holes are 30° apart from the apex. Qualitative features of the conical journal bearing system with hole entry have been elaborated to analyze bearing performance for radial load variation $Wr = 0.25-2$. Numerical results obtained from the present study indicate that load carrying capacity of conical bearing, operating in hydrostatic mode, is enhanced by the maximum pressure, direct fluid film damping and direct film stiffness coefficients vis-a-vis corresponding hybrid mode.

Keywords: Conical journal bearing, CFV restrictor, hole-entry, FEM, Non-recess.

Introduction

Frequent use of journal bearing in various machines led to the development of new and advanced journal bearing so as to give enhanced, more accurate and precise performance. However, the bearing performance is dependent upon the type of bearing, material of bearing, lubricant used and load applied, etc. Presently, conical journal bearings are in use in the industry because it eliminates the use of two separate (radial and thrust) bearings and reduces the vibration in axial and radial direction which provides accuracy in the bearing system. There are various types of conical journal bearings such as hydrodynamic, hybrid and hydrostatic journal bearing. Depending on the type of requirement these bearings are again classified as recessed, non-recessed/without recess and slot entry conical journal bearing. Conical bearings find its use in turbine operating at high speed, mercury paraboloid as reflecting telescope, axial flow blood pump in medical field, precision grinding machine and in precision lathe machine, etc. However, the researchers are continuously striving to investigate new design and configuration of conical journal bearing, to improve the functioning of upcoming machines at higher end. Rowe and Stout [1, 2] is the pioneer in the field of conical bearing. However, Prabhu and Ganesan [3, 4] studied annular

recessed conical hydrostatic thrust bearings ($45^\circ < \gamma < 90^\circ$) with the capillary restrictors for its dynamic behavior. They reported that rotation of lubricant inertia; eccentricity and angle of tilt affect the bearing performance. Nowak and Wierzcholske [5] analyzed the finite width conical bearing using Non-Newtonian lubricant. Khalil [6] analyzed turbulent lubricated externally pressurized conical bearing. Spiral grooved water lubricated conical bearings were studied in hydrostatic mode for high-speed spindles for stability and axial load capacities by Yoshimoto *et al.* [7, 8].

Externally pressurized, porous coated and temperature dependent viscosity conical bearings have been demonstrated by Sinha *et al.* [9] they reported that the porosity affect the inlet pressure and load capacity performance. Practical investigation, for dynamics of carbon epoxy shaft, for conical aerostatic journal bearing with high speed has been carried out by Ingle and Ahuja [10].

When theoretical and experimental work was carried out on conical deep/shallow pocket hybrid bearings, Guo *et al.* [11] demonstrated that the small eccentricity greatly enhanced the stability and load capacity towards the higher end. Sharma *et al.* [12] presented the 4 pocket conical bearing in hydrostatic mode theoretically for the effect of cone angle. They concluded that lubricant flow-rate for the

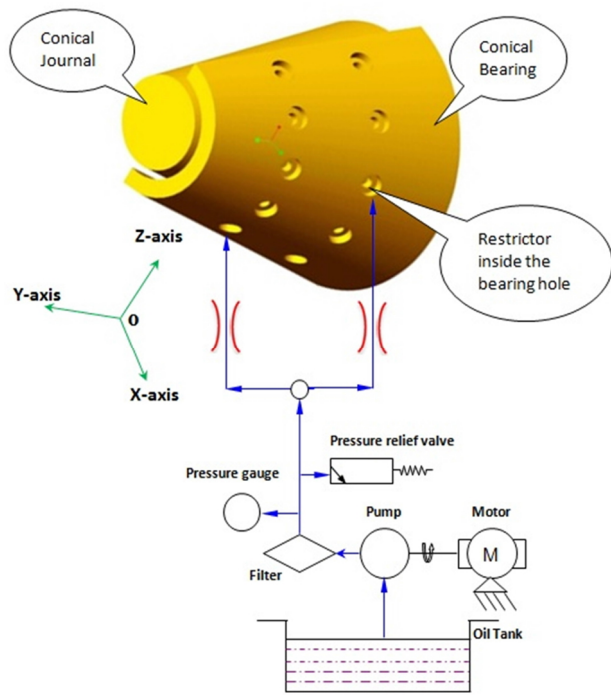


FIGURE 1 Hole-entry hybrid/hydrostatic non-recessed conical journal bearing system

conical bearing was inferior with regards to circular bearing. Sharma *et al.* [13] went ahead with their work to study wear defect on multi recess orifice compensated conical hybrid journal bearing for different semi-cone angles of the bearing. They concluded that wear has affected conical bearing performance to a great extent. Hybrid bearing of conical nature has been analyzed for micropolar lubrication by Sharma and Rajput [14]. They demonstrated the practical use of micropolar fluid for semi cone angle of 10° and 20° . Further, they indicated that micropolar fluids enhance the bearing performance as compared to Newtonian fluid. Korneev [15, 16, 17] studied various conical journal bearings with turbine oil, liquid hydrogen and water as lubricant, where he presented various trajectories and formulae considering turbulence effect. Externally pressurized 4-pocketed conical hybrid journal bearing adjusted for membrane restrictor has been analyzed by Sharma and Rajput [18] using micropolar lubricant. They investigated that the micropolar fluid contributed in increasing fluid film stiffness, dampening coefficient, journal critical speed and threshold speed for stability.

Hydrostatic mode of four-pocketed conical journal bearing, with CFV restrictor and micro-polar fluid, has been theoretically studied by Rana *et al.* [19] they concluded that when there is increase in semi cone angle, radial load and characteristic length, the bearing pressure developed is large. Further, Rajput and Sharma [20] investigated the effect of micropolar fluid on 4 pocketed conical journal bearing adjusted for constant flow valve restrictor in hybrid mode for stability of bearing. They found that the threshold speed using micropolar fluid is enhanced vis-a-vis Newtonian fluid for better bearing stability. Moreover, the film damping and film stiffness coefficient is also influenced

by micropolar fluid. Rana *et al.* [21] theoretically analyzed the 6 pocketed conical bearing adjusted for constant flow valve restrictor in hydrostatic mode for variation in semi cone angles and pockets. They concluded that the conical bearing developed significant pressure, when semi cone angles and number of pockets are increased. Further, 4-pocketed conical journal bearing adjusted for constant flow valve restrictor in hybrid mode have been analytically presented by Rana *et al.* [22] They observed that the critical mass, threshold speed and dynamic characteristics are increased with the increased in restrictor based design parameter and semi cone angle. Extending the research ahead, Rana *et al.* [23] studied the comparison of the CFV compensated 6 pocket and 4 pocket, 20° and 40° conical hybrid journal bearing, in which authors claimed that the 6 pocketed hybrid conical bearing with higher cone angle yielded improved performance than the four pocket hybrid conical journal bearing.

In recent past, Khakse *et al.* [24] presented a hole entry, hybrid, non-recessed conical journal bearing analysis using capillary restrictor for variable load. They concluded that the conical hybrid bearings were indicating better pressure performance for 5° and 10° semi cone bearings. However, the fluid film damping and stiffness performances of conical bearing are also significantly increased with the increased in semi cone angles. Further, Khakse *et al.* [25] extended their study to investigate the semi cone bearing angle influence on non recess conical bearing system with hole entry adjusted for orifice restriction. They found that the minimum fluid film thickness, fluid film stiffness and bearing flow are quite significant in case of hybrid mode corresponding to the conical bearing in hydrostatic mode. As discussed in literature, it could be pointed out that the journal bearings in conical shape have been widely analyzed by the research group of people. However, the analytical study on non-recessed conical hole entry hybrid/ hydrostatic journal bearing with constant flow valve restrictor has not been studied yet, hence, to fill the gap in available literature, performance analysis of conical bearing adjusted for constant flow valve restrictor is undertaken in the present paper.

Theoretical analysis

Non-recessed hybrid/hydrostatic hole entry conical journal bearing adjusted for constant flow valve is depicted in Figure 1, wherein, the performance of conical bearing with hole-entry is to be studied with the help of finite element method and Gauss elimination method. The assumptions made for the new configuration are 1. No slip at the boundaries, 2. Neglecting the body force, 3. Pressure across the thickness remains constant, 4. Inertia effects are neglected, 5. Considering laminar, incompressible and iso-viscous fluid and 6. viscosity is taken as constant throughout the film thickness. The various equations adopted in the analysis are detailed in the following paragraph.

Modified Reynolds Expression

The modified Reynolds expression in spherical coordinates system, regulating the Newtonian lubricant flow in the space between conical journal and bearing with hole-entry, is denoted as [12, 13]:

$$\frac{1}{r} * \frac{\partial}{\partial r} \left(\frac{r}{12\mu} h^3 \frac{\partial p}{\partial r} \right) + \frac{1}{\sin^2 \gamma} * \frac{\partial}{\partial \varphi} \left(\frac{h^3}{12\mu r^2} \frac{\partial p}{\partial \varphi} \right) = \frac{\omega_j}{2} \frac{\partial h}{\partial \varphi} + \frac{\partial h}{\partial t} \quad (1)$$

Subjecting following non-dimensional parameters in the Eq.(1)

$$\bar{p} = \frac{p}{p_s}; \beta = r \sin \gamma / R_j; \bar{h} = \frac{h}{c}; \bar{t} = \frac{t}{\left[\frac{\mu R_j^2}{c^2 p_s} \right]}$$

($\alpha = \varphi$) is the non-dimensional coordinate (Angular measure is in radian).

The modified Reynolds expression in which, isoviscous, incompressible, laminar lubricant flow is controlled in the space of journal and bearing. It is expressed in non-dimensional term as [12, 13]:

$$\frac{\partial}{\partial \alpha} \left[\left(\frac{1}{\beta} \right) \frac{\bar{h}^3}{12\bar{\mu}} \frac{\partial \bar{p}}{\partial \alpha} \right] + \frac{\partial}{\partial \beta} \left[\sin^2 \gamma * (\beta) \frac{\bar{h}^3}{12\bar{\mu}} \frac{\partial \bar{p}}{\partial \beta} \right] = \frac{\Omega}{2} \frac{\partial \bar{h}}{\partial \alpha} + \beta \frac{\partial \bar{h}}{\partial \bar{t}} \quad (2)$$

Constant Flow Valve Based Restrictor Equation

A compensator/restrictor is introduced in the bearing with hole-entry, to allow fluid supply in the space between two conical mating parts, with the intension of controlling the fluid flow which supplies fixed quantity of flow. The fluid flowing through (CFV) constant flow valve adjusted hydrostatic/hybrid conical journal bearing, in non-dimensional terms, is expressed as [26]:

$$\bar{Q}_R = \bar{Q}_c = \text{constant} \quad (3)$$

Where, \bar{Q}_c = given flow rate in the restrictor.

Fluid Film Thickness

To operate conical bearing without the friction and wear, bearing surfaces are fully lubricated with lubricant; this lubricant is allowed to maintain certain thickness called insignificantly small fluid film thickness (h). Normally, this film thickness for conical journal bearing with hole-entry is formulated in non-dimensional terms as [11]:

$$\bar{h}_0 = -\cos \gamma (\bar{X}_j \cos \alpha + \bar{Z}_j \sin \alpha - 1) \quad (4)$$

Finite Element Method (FEM) Formulation

The geometry of mesh grid of lubricant fluid flow for non-recess conical journal bearing with hole-entry system in hybrid/hydrostatic mode has been presented in figure 2. Bearing system clearance flow field is divided into many

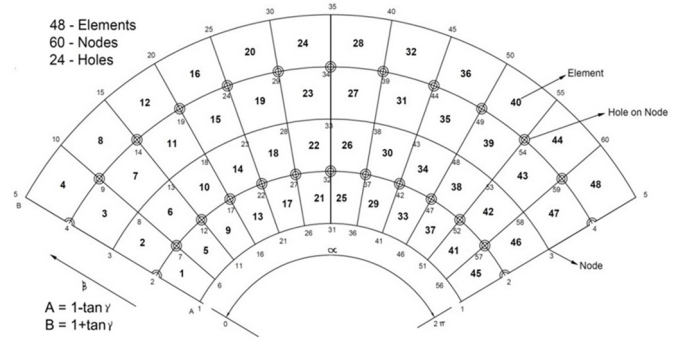


FIGURE 2 Meshing of lubricant flow field

isoparametric elements, having four nodes to each element, for simplicity and feasibility of the solution; else, elements with different node numbers could have been adopted. Lagrangian interpolation function is applied to isoparametric element to find pressure at required location in isoparametric element. This is elaborated as:

$$\sum_{j=1}^4 N_j \bar{p}_j = \bar{p} \quad (5a)$$

Where, N_j = elemental shape function, it can be expressed in co-ordinates locally as:

$$N_1 = \frac{1}{4} (1-\xi)(1-\eta); N_2 = \frac{1}{4} (1+\xi)(1-\eta) \\ N_3 = \frac{1}{4} (1+\xi)(1+\eta); N_4 = \frac{1}{4} (1-\xi)(1+\eta) \quad (5b)$$

$$\bar{p}^e = [N_1, N_2, N_3, N_4] \begin{Bmatrix} \bar{p}_1 \\ \bar{p}_2 \\ \bar{p}_3 \\ \bar{p}_4 \end{Bmatrix} \quad (5c)$$

Galerkin's technique with orthogonality terms are applied to Eq. (2) with the approximate pressure value \bar{p} from Eq. (5a).

$$\frac{\partial}{\partial \alpha} \left[\left(\frac{1}{\beta} \right) * \frac{\bar{h}^3}{12\bar{\mu}} * \frac{\partial}{\partial \alpha} \sum_{j=1}^4 N_j \bar{p}_j \right] + \frac{\partial}{\partial \beta} \left[\sin^2 \gamma * (\beta) * \frac{\bar{h}^3}{12\bar{\mu}} * \frac{\partial}{\partial \beta} \sum_{j=1}^4 N_j \bar{p}_j \right] - \frac{\Omega}{2} \frac{\partial \bar{h}}{\partial \alpha} - \beta \frac{\partial \bar{h}}{\partial \bar{t}} = R^e \quad (6)$$

Where "R^e" = Residue.

After simplification the typical elemental matrix equation resulted as [26]:

$$\begin{aligned} & \{Q\}^e + \Omega \{R_H\}^e + \bar{X}_J \{R_{XJ}\}^e + \bar{Z}_J \{R_{ZJ}\}^e \\ & = [F]^e \{\bar{p}\}^e \end{aligned} \quad (7a)$$

Where, e^{th} element can be elaborated as:

$$\begin{aligned} \bar{F}_{ij}^e = \iint_{A^e} & \frac{\bar{h}^3}{12} \left[\frac{\partial N_i}{\partial \alpha} \frac{\partial N_j}{\partial \alpha} * \frac{1}{\sin \gamma} \right. \\ & + \sin \gamma (\beta^2) \\ & \left. * \frac{\partial N_i}{\partial \beta} \frac{\partial N_j}{\partial \beta} \right] d\alpha d\beta \end{aligned} \quad (7b)$$

$$\begin{aligned} \bar{Q}_i^e = \int_{\Gamma^e} & \left\{ \left(\frac{\bar{h}^3}{12} \frac{\partial \bar{p}}{\partial \alpha} - \frac{\Omega}{2} \bar{h} \right) \frac{1}{\sin \gamma} l_1 \right. \\ & + \sin \gamma (\beta^2) \\ & \left. * \left(\frac{\bar{h}^3}{12} \frac{\partial \bar{p}}{\partial \beta} \right) l_2 \right\} N_i d\Gamma^e \end{aligned} \quad (7c)$$

$$\bar{R}_{Hi}^e = \iint_{A^e} \frac{\bar{h}}{2} \frac{\partial N_i}{\partial \alpha} * \left(\frac{\beta}{\sin \gamma} \right) d\alpha d\beta \quad (7d)$$

$$\bar{R}_{XJi}^e = \iint_{A^e} N_i \left(\frac{\beta^2}{\sin \gamma} \right) * \cos \alpha * \cos \gamma d\alpha d\beta \quad (7e)$$

$$\bar{R}_{ZJi}^e = \iint_{A^e} N_i \left(\frac{\beta^2}{\sin \gamma} \right) * \sin \alpha * \cos \gamma d\alpha d\beta \quad (7f)$$

l_1 and l_2 denotes direction cosines.

$i, j = 1, 2, \dots, n_i^e$ are the elemental local node numbers.

A^e is the domain of field and Γ^e is the e^{th} elemental boundary.

Further, the element matrices are assembled together and it is denoted as global matrix [26]:

$$\{Q\} + \Omega \{R_H\} + \bar{X}_J \{R_{XJ}\} + \bar{Z}_J \{R_{ZJ}\} = [F] \{\bar{p}\} \quad (8)$$

where,

- $\{Q\}$ = Flow vector for nodes,
- $[F]$ = Assembly of fluidity Matrix,
- $\{R_H\}$ = Column vector for hydro-dynamic terms,

$\{R_{XJ}\}, \{R_{ZJ}\}$ = Global vectors for journal center linear velocities at right hand side

$\{\bar{p}\}$ = pressure vector for nodes,

Further expansion of the equation (8) can be written as follows:

$$\begin{pmatrix} \bar{p}_1 \\ \bar{p}_i \\ \bar{p}_j \\ \bar{p}_n \end{pmatrix} \begin{pmatrix} \bar{F}_{11} & \bar{F}_{1i} & \bar{F}_{1j} & \bar{F}_{1n} \\ \bar{F}_{i1} & \bar{F}_{ii} & \bar{F}_{ij} & \bar{F}_{in} \\ \bar{F}_{j1} & \bar{F}_{ji} & \bar{F}_{jj} & \bar{F}_{jn} \\ \bar{F}_{n1} & \bar{F}_{ni} & \bar{F}_{nj} & \bar{F}_{nn} \end{pmatrix} \quad (9)$$

$$= \begin{pmatrix} \bar{Q}_1 \\ \bar{Q}_i \\ \bar{Q}_j \\ \bar{Q}_n \end{pmatrix} + \begin{pmatrix} \bar{R}_{H1} \\ \bar{R}_{Hi} \\ \bar{R}_{Hj} \\ \bar{R}_{Hn} \end{pmatrix} \Omega$$

$$+ \begin{pmatrix} \bar{R}_{x1} \\ \bar{R}_{xi} \\ \bar{R}_{xj} \\ \bar{R}_{xn} \end{pmatrix} \bar{x} + \begin{pmatrix} \bar{R}_{z1} \\ \bar{R}_{zi} \\ \bar{R}_{zj} \\ \bar{R}_{zn} \end{pmatrix} \bar{z}$$

where, $\{\bar{F}_{ij}\}$ is matrix and $\{\bar{Q}\}, \{\bar{R}_H\}, \{\bar{R}_{XJ}\}, \{\bar{R}_{ZJ}\}$ are column vectors

Now, to the pressure specific, let j^{th} point be the pressure in the fluid flow field as:

$$\bar{p}_j = \bar{p}_j (\bar{X}_J, \bar{Z}_J, \bar{Z}_J, \bar{X}_J) \quad (10)$$

Equation (10) indicates that the pressure is dependent upon the conical journal center's steady state and dynamic condition. The equation (10) is simplified to obtain the steady state condition as follow.

$$\bar{p}_j = \bar{p}_j (\bar{X}_J, \bar{Z}_J) = \bar{p}_o$$

where, \bar{p}_o = steady state pressure at node.

Now, for the flow of fluid to be continuous through the conical bearing adjusted for constant flow valve restrictor, the equation (9) is modified for j^{th} node using the equation- (3) which replaces \bar{Q}_j as $\bar{Q}_R = \bar{Q}_j = \bar{Q}_c$ and leads to the equation- (11).

$$\begin{pmatrix} \bar{p}_1 \\ \bar{p}_i \\ \bar{p}_j \\ \bar{p}_n \end{pmatrix} \begin{pmatrix} \bar{F}_{11} & \bar{F}_{1i} & \bar{F}_{1j} & \bar{F}_{1n} \\ \bar{F}_{i1} & \bar{F}_{ii} & \bar{F}_{ij} & \bar{F}_{in} \\ \bar{F}_{j1} & \bar{F}_{ji} & \bar{F}_{jj} & \bar{F}_{jn} \\ \bar{F}_{n1} & \bar{F}_{ni} & \bar{F}_{nj} & \bar{F}_{nn} \end{pmatrix} = \begin{pmatrix} \bar{Q}_1 \\ \bar{Q}_i \\ \bar{Q}_j = \bar{Q}_R = \bar{Q}_c \\ \bar{Q}_n \end{pmatrix} \quad (11)$$

$$+ \begin{pmatrix} \bar{R}_{H1} \\ \bar{R}_{Hi} \\ \bar{R}_{Hj} \\ \bar{R}_{Hn} \end{pmatrix} \Omega + \begin{pmatrix} \bar{R}_{x1} \\ \bar{R}_{xi} \\ \bar{R}_{xj} \\ \bar{R}_{xn} \end{pmatrix} \bar{x} + \begin{pmatrix} \bar{R}_{z1} \\ \bar{R}_{zi} \\ \bar{R}_{zj} \\ \bar{R}_{zn} \end{pmatrix} \bar{z}$$

Equation - (11) then simplified to get pressure at hole or node with the boundary conditions as below.

Boundary Conditions for flow field

Lubricant flow field is analyzed for the boundary conditions as mentioned below [25]:

- 1) Lubricant passing through compensator is equivalent as hole input flow.
- 2) The nodal flows are non-zero for external boundaries and nodes on holes except at internal nodes.
- 3) Relative pressure equal to zero for conical bearing having boundary nodes open to atmospheric pressure, $\bar{p}|_{\beta=\pm 1.0} = \mathbf{0.0}$
- 4) Trailing edge of the flow field in positive region is subjected to Reynolds boundary condition i.e. $\bar{p} = \frac{\partial \bar{p}}{\partial \alpha} = \mathbf{0.0}$

Stiffness and Damping Coefficient of the Fluid Film

As the film thickness changes, it intends to change the fluid film reaction negatively, the phenomenon is termed as coefficient of fluid-film stiffness and is described as follow:

$$-\frac{\partial \bar{F}_i}{\partial \bar{q}_j} = \bar{S}_{ij}, \quad (i = X, Z) \quad (12a)$$

where,

\bar{q}_j = journal centre displacement direction in \bar{X}_j, \bar{Z}_j axes.

i = moment direction or force.

The matrix form of the stiffness coefficients:

$$\begin{bmatrix} \bar{S}_{XX} & \bar{S}_{XZ} \\ \bar{S}_{ZX} & \bar{S}_{ZZ} \end{bmatrix} = - \begin{bmatrix} \frac{\partial \bar{F}_X}{\partial \bar{X}_j} & \frac{\partial \bar{F}_X}{\partial \bar{Z}_j} \\ \frac{\partial \bar{F}_Z}{\partial \bar{X}_j} & \frac{\partial \bar{F}_Z}{\partial \bar{Z}_j} \end{bmatrix} \quad (12b)$$

The damping coefficient of fluid-film is the negative rate change in fluid film reaction for journal centre velocity in coordinate directions. It is expressed as:

$$\bar{C}_{ij} = -\frac{\partial \bar{F}_i}{\partial \bar{q}_j}, \quad (i = X, Z) \quad (13a)$$

where, \bar{q}_j = journal centre velocity component along \bar{X}_j, \bar{Z}_j directions.

Similarly, the matrix of the damping coefficients:

$$\begin{bmatrix} \bar{C}_{XX} & \bar{C}_{XZ} \\ \bar{C}_{ZX} & \bar{C}_{ZZ} \end{bmatrix} = - \begin{bmatrix} \frac{\partial \bar{F}_X}{\partial \dot{\bar{X}}_j} & \frac{\partial \bar{F}_X}{\partial \dot{\bar{Z}}_j} \\ \frac{\partial \bar{F}_Z}{\partial \dot{\bar{X}}_j} & \frac{\partial \bar{F}_Z}{\partial \dot{\bar{Z}}_j} \end{bmatrix} \quad (13b)$$

Thus, the coefficient for fluid film damping $\bar{C}_{ij}(i = \bar{X}_j, \bar{Z}_j)$ can be found by mathematical operation on equation -(8).

Solution procedure

Iterative procedure is applied to obtain the lubricant flow field solution with presumption that the steady state consideration and viscosity is constant (i.e. zero value of velocity component of the journal centre). This led to the use of only journal centre coordinates (\bar{X}_j, \bar{Z}_j) in equation-(8) and the solution can be obtained by Gauss elimination method. Feedback loop to this iterative scheme is also developed for equilibrium to be maintained using following equations:

$$\bar{F}_X = 0 \quad \text{and} \quad \bar{F}_Z - \bar{W}_r = 0 \quad (14)$$

i^{th} journal centre position can be found out by applying Taylor's series to equation- (14) with following increment ($\Delta \bar{X}_j^i, \Delta \bar{Z}_j^i$) of the journal.

where,

$$\Delta \bar{X}_j^i = -\frac{1}{D_j} \left[\frac{\partial \bar{F}_Z}{\partial \bar{Z}_j} \Big|_i - \frac{\partial \bar{F}_X}{\partial \bar{Z}_j} \Big|_i \right] \left\{ \frac{\bar{F}_X^i}{\bar{F}_Z^i - \bar{W}_r} \right\} \quad (15a)$$

$$\Delta \bar{Z}_j^i = -\frac{1}{D_j} \left[-\frac{\partial \bar{F}_Z}{\partial \bar{X}_j} \Big|_i \frac{\partial \bar{F}_X}{\partial \bar{X}_j} \Big|_i \right] \left\{ \frac{\bar{F}_X^i}{\bar{F}_Z^i - \bar{W}_r} \right\} \quad (15b)$$

in which,

$$D_j = \left(\frac{\partial \bar{F}_X}{\partial \bar{X}_j} \Big|_i \cdot \frac{\partial \bar{F}_Z}{\partial \bar{Z}_j} \Big|_i - \frac{\partial \bar{F}_X}{\partial \bar{Z}_j} \Big|_i \cdot \frac{\partial \bar{F}_Z}{\partial \bar{X}_j} \Big|_i \right) \quad (15c)$$

Thus, the immediate subsequent journal centre coordinates ($\bar{X}_j^{i+1}, \bar{Z}_j^{i+1}$) are represented as:

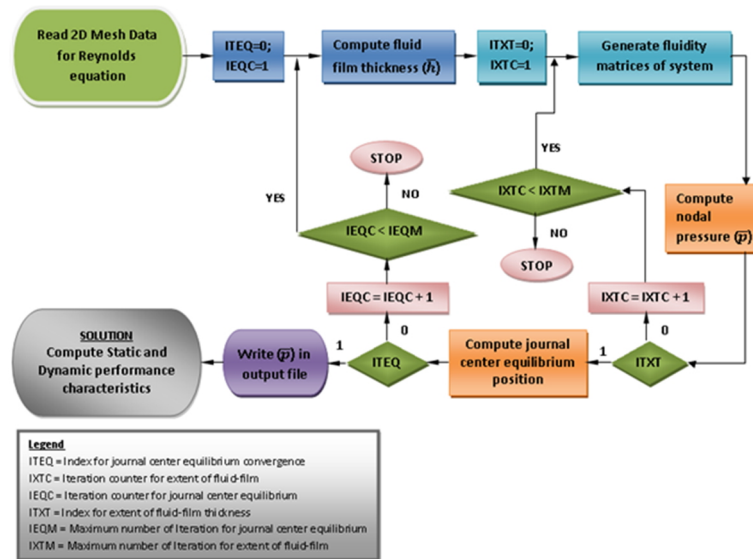


FIGURE 3 Iteration flow chart.

$$\bar{X}_j^i + \Delta \bar{X}_j^i = \bar{X}_j^{i+1} \quad (16a)$$

$$\bar{Z}_j^i + \Delta \bar{Z}_j^i = \bar{Z}_j^{i+1} \quad (16b)$$

Where, journal centre position coordinate = \bar{X}_j^i, \bar{Z}_j^i

Iterative solution is carried forward till the following convergence standard is obtained. After attaining the convergence standard, necessary static characteristics in terms of maximum pressure, bearing fluid flow, minimum fluid film thickness and dynamic performance characteristics in terms of damping, stiffness and threshold speed can be found out.

$$\left[\frac{((\Delta \bar{X}_j^i)^2 + (\Delta \bar{Z}_j^i)^2)^{1/2}}{((\bar{X}_j^i)^2 + (\bar{Z}_j^i)^2)^{1/2}} \right] \times 100 < 0.001 \quad (17)$$

Step by step solution for iterative scheme is as in Figure 3.

Results and discussion

Static performance curve and dynamic performance curve of non-recessed conical journal bearing with hole entry adjusted for constant flow valve in hydrostatic/hybrid modes are found out by soft skill coding in Fortran 77. The subject bearing configuration consisting of variations in semi cone angles with the holes in double row on the bearing circumference, in which 12 equidistant holes are located in each row circumferentially. Various bearing parameter in terms of operation and its geometry are listed in table-1. However, the bearing performance is analyze for semi cone bearing angle (γ) = 5°, 10°, 20° and 30° for radially loaded range $\bar{W}_r = 0.25 - 2$. Thorough scan did not reveal the availability of theoretical or experimental results on constant flow valve adjusted hole-entry hydrostatic/hybrid conical journal bearing. Rowe dealt

Table 1. Parameters under consideration for conical journal bearing with hole-entry:

Parameters for Bearing	Notation and symbol	Values
Bearing aspect ratio	λ	1.0
Ratio of concentric design pressure	β^*	0.5
Radially loaded Externally	\bar{W}_r	0.25 - 2
holes	n	12
Land width ratio	\bar{a}_b	0.25
Rows	—	2
Restrictor used	—	Constant flow valve
Speed parameter	Ω	1 = (Hybrid) 0 = (Hydrostatic)
Bearings with different semi cone angle γ		
No.1 Bearing		$\gamma = 5^\circ$
No.2 Bearing		$\gamma = 10^\circ$
No.3 Bearing		$\gamma = 20^\circ$
No.4 Bearing		$\gamma = 30^\circ$

most of the work on hydrostatic/hybrid conical journal bearing thus, the results of present paper have been compared with the Stout and Rowe [1] published results, which indicate close agreement of the comparison as depicted in figure 4.

Change in pressure (\bar{p}_{max}) versus load (\bar{W}_r) in radial direction

Figure 5(a) shows the variation of maximum pressure (\bar{p}_{max}) for change of radial load (\bar{W}_r) for constant flow valve adjusted non-recess conical journal bearing with hole-entry

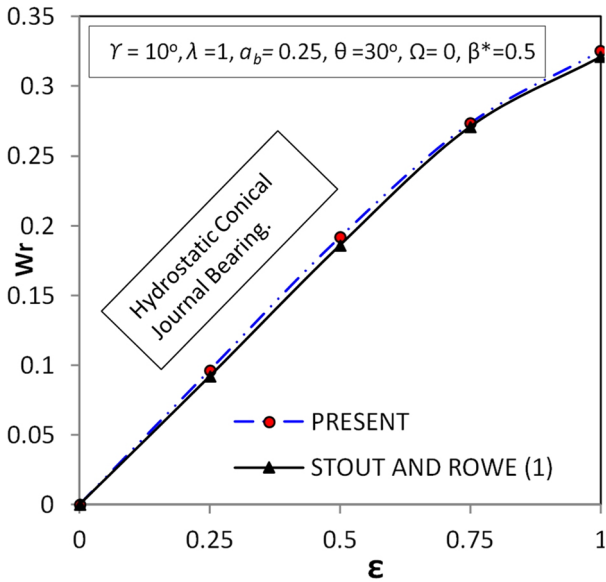


FIGURE 4 Load in radial direction (\bar{W}_r) versus eccentricity ratio (ϵ).

in hybrid/hydrostatic mode. It has been observed that the \bar{p}_{max} is increased when there is increased in radial load \bar{W}_r for bearing operating in both hybrid and hydrostatic mode. Further, the non-recess conical bearing with hole-entry indicate better performance in hydrostatic mode as compared to the hybrid mode for all semi cone angles (γ) journal bearings. However, conical journal bearing in hydrostatic mode indicate more prominent max. pressure for radial loading \bar{W}_r at the nascent stage than the counterpart in hybrid mode. Both the bearing operating mode show monotonic behavior. It was noticed that the conical bearing in hydrostatic mode follows little curvilinear route; this is because of the varying nature pressure pattern due to constant flow valve restrictor. Observation indicate that the increase in semi cone bearing angle from $\gamma = 5^\circ$ to 30° , increases max. pressure \bar{p}_{max} also. Semi cone angle $\gamma = 30^\circ$ shows higher \bar{p}_{max} for conical bearing with hydrostatic and hybrid mode of operation. So, it is preferable to use constant flow valve hole-entry conical bearing for higher load \bar{W}_r , so that maximum pressure can be achieved. While the hole-entry conical bearing is made to operate at $\bar{W}_r = 2.0$, the change in percentage of \bar{p}_{max} with respect to 5° base bearing operating in hybrid mode, is found to be of the order of -0.04 %, 4.55 % and 12.79 % for $\gamma = 10^\circ$, 20° , and 30° semi cone angle respectively. Likewise, the percentage change in conical journal bearing operating in hydrostatic mode with respect to hybrid mode, for the similar semi cone angles and radial loading, is noticed of the order of 22.02 %, 23.71 %, 25.13 %, and 27.73 % for $\gamma = 5^\circ$, 10° , 20° and 30° semi-cone angle bearings respectively. Profile of pressure for conical journal bearing with hole-entry operating in hybrid and hydrostatic mode is as shown in Figure 5(b) and 5(c) respectively. This pressure profile indicates the real time pressure at every angle during the performance.

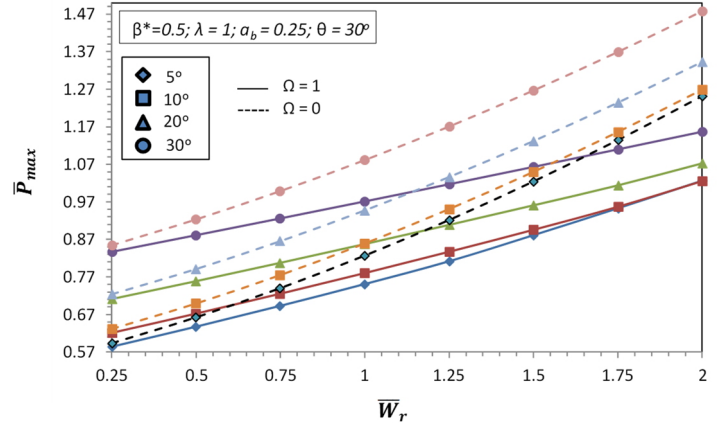


FIGURE 5(a) Change in pressure (\bar{p}_{max}) versus load (\bar{W}_r) in radial direction

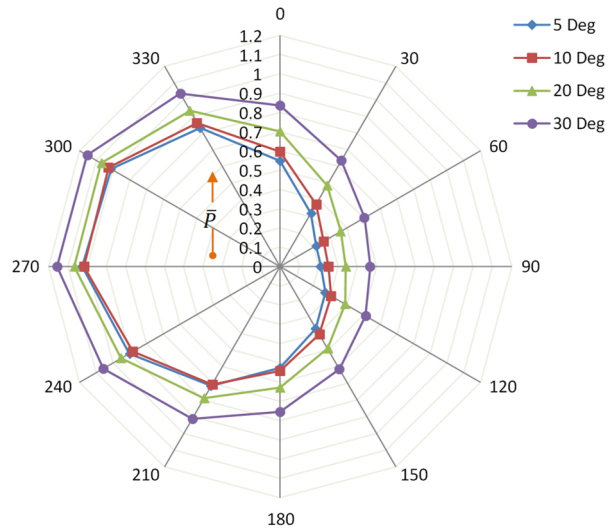


FIGURE 5(b) Circumferential profile of pressure, for CFV compensated conical journal bearing with hole-entry in hybrid mode, for different semi cone angles at $\bar{W}_r = 2$.

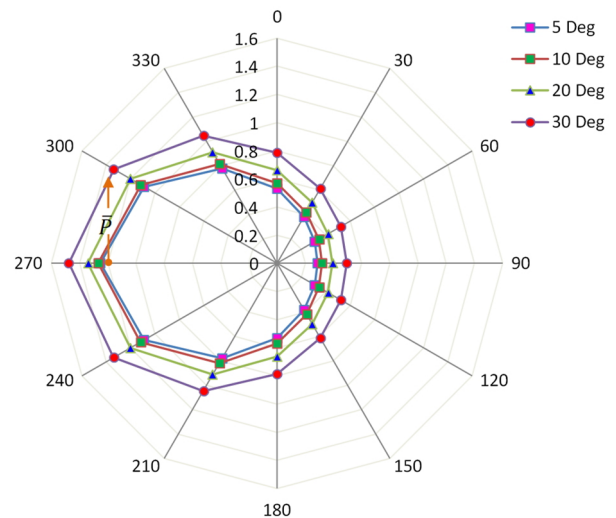


FIGURE 5(c) Circumferential profile of pressure, for CFV compensated conical journal bearing with hole-entry in hydrostatic mode, for different semi cone angles at $\bar{W}_r = 2$.

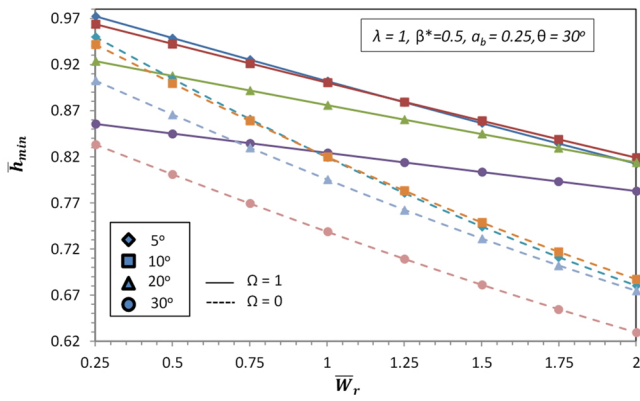


FIGURE 6 Change in fluid film thickness (\bar{h}_{min}) versus load (\bar{W}_r) in radial direction

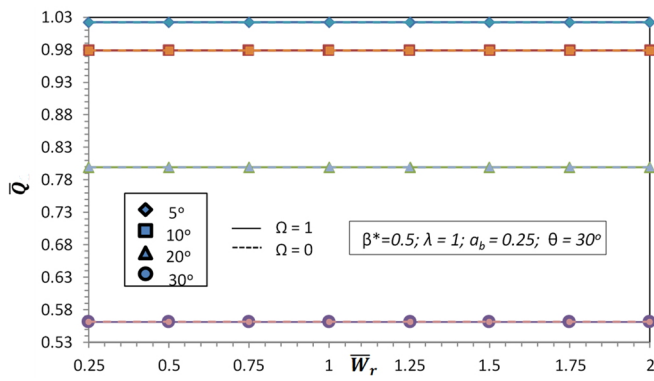


FIGURE 7 Change in bearing flow (\bar{Q}) versus load (\bar{W}_r) in radial direction

Change in fluid film thickness (\bar{h}_{min}) versus load (\bar{W}_r) in radial direction

Figure 6 depicts the change in minimal thickness of fluid film (\bar{h}_{min}) for varying load (\bar{W}_r) in radial direction for semi cone bearing angle from $\gamma = 5^\circ$ to 30° . It has been pointed out that, as the radial load \bar{W}_r is increased, \bar{h}_{min} is decreased in hybrid and hydrostatic mode; this is due to increasing application of radial load. Further, the decrease in \bar{h}_{min} is observed to be less in conical bearing operating in hybrid mode corresponding to hydrostatic mode, because journal speed assists in developing additional pressure and hence sufficiently higher \bar{h}_{min} is maintained for the same radial load \bar{W}_r . Furthermore, Figure 6 also indicate that the increased in semi cone angle leads to decrease in \bar{h}_{min} in both the operating modes. It is interesting to note that the performance of hybrid as well as hydrostatic hole-entry bearings are almost similar for the application of radial load $\bar{W}_r = 0.95$ to 1.25 for $\gamma = 5^\circ$ and 10° . It is desirable to have higher \bar{h}_{min} , hence semi cone angle $\gamma = 5^\circ$ and 10° journal bearing operating in hybrid and hydrostatic mode, adjusted for constant flow valve, are suitable for the desired and higher performance. Hence, it is recommended to go for lower range of radial load \bar{W}_r to obtain the higher \bar{h}_{min} . During operation of conical bearing in hybrid mode at $\bar{W}_r = 2.0$, the percentage change in \bar{h}_{min} with reference to $\gamma = 5^\circ$ base bearing, is noted of the order of 0.79 %, 0.16 % and -3.67 % for $\gamma = 10^\circ, 20^\circ$ and 30° conical bearings respectively.

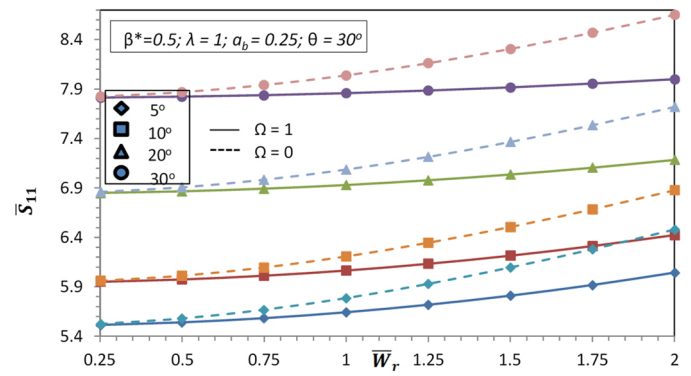


FIGURE 8 Change in direct fluid film stiffness (\bar{S}_{11}) coefficient versus load (\bar{W}_r) in radial direction

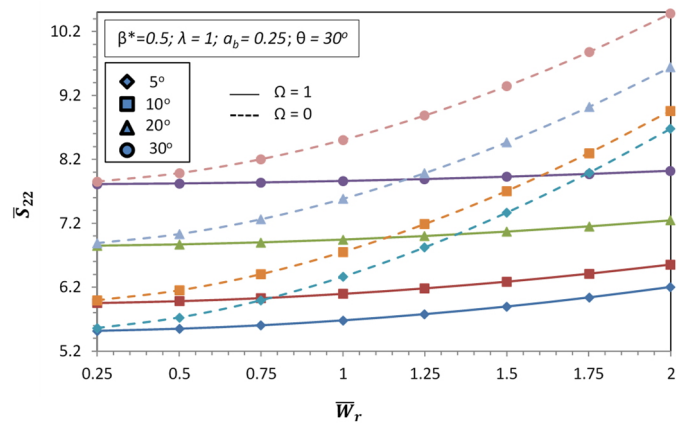


FIGURE 9 Change in direct fluid film stiffness (\bar{S}_{22}) coefficient versus load (\bar{W}_r) in radial direction.

Likewise, percentage change in conical journal bearing operating in hybrid mode with respect to hydrostatic mode, for the similar semi cone angles and radial loading, is noticed of the order of 19.5 %, 19.14 %, 20.66 %, and 24.39 % for $\gamma = 5^\circ, 10^\circ, 20^\circ$ and 30° semi-cone angle bearings respectively.

Change in bearing flow (\bar{Q}) versus load (\bar{W}_r) in radial direction

Figure 7 indicate the change in flow through bearing (\bar{Q}) with respect to the load in radial direction (\bar{W}_r) for different semi cone bearing angles (γ). Since the non-recess conical journal bearings with hole-entry, operating in hybrid and hydrostatic mode, are employed with the constant flow valve restrictors, these show constant flow through different cone angle bearings for all radially loaded (\bar{W}_r) conditions. When the bearing cone angle is raised corresponding flow \bar{Q} through bearing is found to be decreased. However, the semi cone angle $\gamma = 5^\circ$ show the higher bearing flow operating in hydrostatic and hybrid modes. While the conical bearing with hole-entry is made to operate at $\bar{W}_r = 2.0$, the change in percentage of bearing flow (\bar{Q}) for $\gamma = 10^\circ, 20^\circ$ and 30° semi-cone angles with respect to 5° base bearing operating in hybrid mode, is observed to be of the order of -4.22 %, -21.83 % and -45.07 % respectively.

Change in direct fluid film stiffness (\bar{S}_{11}) coefficient versus load (\bar{W}_r) in radial direction

Figure 8 depicts the graph for coefficient of direct fluid film stiffness (\bar{S}_{11}) versus loading in radial direction (\bar{W}_r) for $\gamma = 5^\circ, 10^\circ, 20^\circ$ and 30° cone angle bearings. The observation is made from figure 8 that when the bearing (\bar{W}_r) radial load is increased, the coefficient of direct fluid film stiffness \bar{S}_{11} is also increased when operated at hydrostatic and hybrid mode. The increase in stiffness coefficient (\bar{S}_{11}) is found to be higher in hole-entry conical journal bearing operating at hydrostatic mode than the hybrid mode. When bearing semi cone angle is raised from $\gamma = 5^\circ, 10^\circ, 20^\circ$ and 30° , the stiffness coefficient, too, is found to be increased.

It is also noticed that the larger increase in stiffness coefficient (\bar{S}_{11}) could be achieved near the extremely higher loading (\bar{W}_r) when operated in hydrostatic mode. Whereas, at the initial radial loading on conical bearing, the almost similar stiffness coefficient could be observed in both the hybrid and hydrostatic modes. When the conical bearing angle is increased from $\gamma = 5^\circ$ to 30° , the stiffness is also increased but, the increase in stiffness is not that much for $\gamma = 30^\circ$ in hybrid mode. However, the semi cone angle bearing $\gamma = 30^\circ$ shows higher bearing stiffness coefficient (\bar{S}_{11}) when operated in hydrostatic mode. During operation of conical bearing in hybrid mode at $\bar{W}_r = 2.0$, the percentage change in (\bar{S}_{11}) with reference to $\gamma = 5^\circ$ base bearing, is noted of the order of 6.30 %, 18.88 % and 32.38 % for $\gamma = 10^\circ, 20^\circ$ and 30° conical bearings respectively. Likewise, the percentage change in (\bar{S}_{11}) for conical bearing operating in hydrostatic mode with respect to hybrid mode, for the similar angles and radial loading, is observed of the order of 7.21 %, 7.05 %, 7.46 % and 8.13 % for $\gamma = 5^\circ, 10^\circ, 20^\circ$ and 30° semi-cone angle bearings respectively.

Change in direct fluid film stiffness (\bar{S}_{22}) coefficient versus load (\bar{W}_r) in radial direction

Influences of direct fluid film stiffness coefficient (\bar{S}_{22}) for different semi cone angle bearings (γ) are as shown in figure 9. It has been noticed from figure 9 that the stiffness coefficient (\bar{S}_{22}) of conical bearing is increased when radial loading (\bar{W}_r) is increased, while operating in hybrid and hydrostatic mode. The increase in stiffness coefficient (\bar{S}_{22}) is found to be higher for bearing operating in hydrostatic mode when compared with hybrid mode, this is because, the contour of the conical bearing and step up application of load, the pressure available in clearance increases which helps in stiffening the bearing. However, the stiffness coefficient is far better for at higher radial load \bar{W}_r in hydrostatic case.

Observation is also made that when the hole-entry semi cone bearing angle is increased from $\gamma = 5^\circ$ to 30° , the stiffness coefficient \bar{S}_{22} is also increased while operating in hybrid and hydrostatic mode. However, semi cone angle $\gamma = 30^\circ$ indicates higher film stiffness in hydrostatic case. While the hole-entry conical bearing is made to operate at $\bar{W}_r = 2.0$, the change in percentage in (\bar{S}_{22}) with reference to 5° base bearing operating in hybrid mode, is noted of the order of 5.66 %, 16.85 % and 29.33 % for $\gamma = 10^\circ, 20^\circ$ and 30°

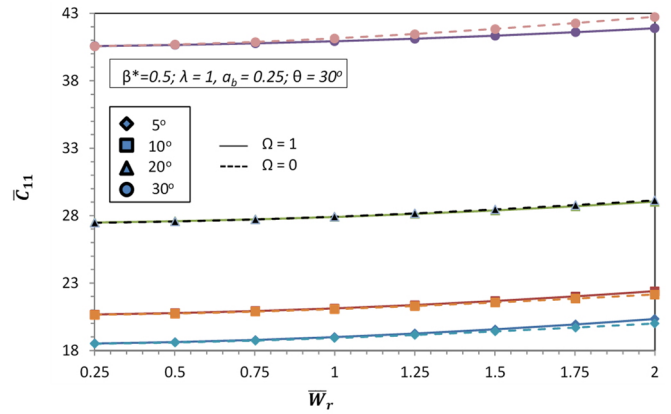


FIGURE 10 Change in direct fluid film damping (\bar{C}_{11}) coefficient versus load (\bar{W}_r) in radial direction.

semi cone angle bearings respectively. Likewise, the percentage change in (\bar{S}_{22}) for bearing working in hydrostatic mode with reference to hybrid mode, for the similar semi cone angles and radial loadings, is found of the order of 39.94 %, 36.72 %, 33.05 %, and 30.69 % for semi-cone angles $\gamma = 5^\circ, 10^\circ, 20^\circ$ and 30° respectively.

Change in direct fluid film damping (\bar{C}_{11}) coefficient versus load (\bar{W}_r) in radial direction.

Change in fluid film damping (\bar{C}_{11}) coefficient versus load (\bar{W}_r) in radial direction has been demonstrated for $\gamma = 5^\circ, 10^\circ, 20^\circ$ and 30° bearings in figure 10. It has been observed while the bearing was operating in hybrid and hydro-static mode that when the bearing cone angle is modified in steps from $\gamma = 5^\circ$ to 30° , the fluid film damping (\bar{C}_{11}) coefficient is also significantly modified. However, semi cone angle $\gamma = 30^\circ$ bearing show higher damping performance in hydrostatic mode. In addition to that, the damping coefficient (\bar{C}_{11}) performance is also increased as the radial load \bar{W}_r is increased. It is important to note that the damping leads in performance at extreme range of loads in hybrid mode for bearing with $\gamma = 5^\circ$ and 10° . Whereas, the damping leads in performance at extreme load range in hydrostatic mode for bearing with $\gamma = 30^\circ$ and onwards. The damping is almost similar in both hydrostatic and hybrid mode throughout the load variation for bearing with $\gamma = 20^\circ$. It has been found that the overall damping performance (\bar{C}_{11}) of the conical journal bearings, operating in both hydrostatic and hybrid mode, are very much close. When the hole-entry conical bearing is made to operate at $\bar{W}_r = 2.0$, the change in percentage of (\bar{C}_{11}) with respect to 5° base bearing operating in hybrid mode, is observed of the order of 10.06 %, 42.72 % and 105.96 % for $\gamma = 10^\circ, 20^\circ$ and 30° bearings respectively. Likewise, the percentage change in (\bar{C}_{11}) for conical journal bearing operating in hybrid mode with reference to hydrostatic mode, for the similar semi cone angles and radial loading, is found of the order of 1.70 %, 1.09 %, -0.35 % and -1.96 % for the bearings with $\gamma = 5^\circ, 10^\circ, 20^\circ$ and 30° respectively.

Change in direct fluid film damping (\bar{C}_{22}) coefficient versus load (\bar{W}_r) in radial direction

Influence of various semi cone bearing angles $\gamma = 5^\circ,$

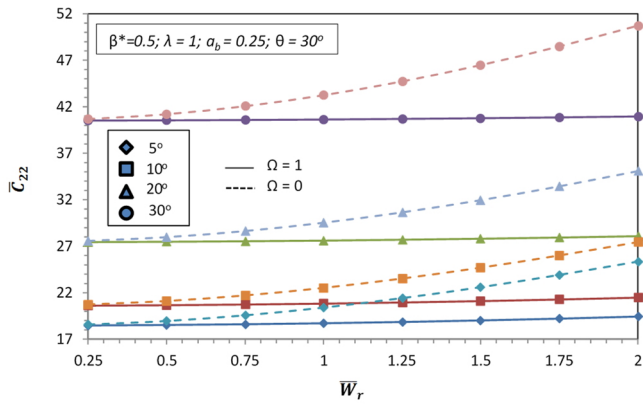


FIGURE 11 Change in direct fluid film damping (\bar{C}_{22}) coefficient versus load (\bar{W}_r) in radial direction

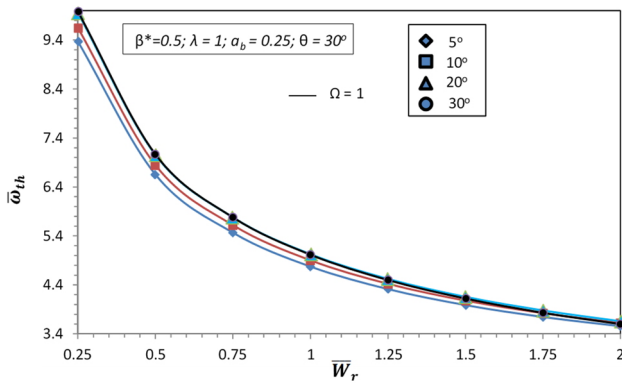


FIGURE 12 Threshold speed ($\bar{\omega}_{th}$) change versus load (\bar{W}_r) in radial direction

10°, 20° and 30° on direct damping (\bar{C}_{22}) coefficient for radially loaded (\bar{W}_r) condition have been presented in figure 11. Damping (\bar{C}_{22}) coefficient of conical hole entry journal bearings are higher at extreme loading in hydrostatic mode. Whereas, all semi cone angles (γ) hole entry journal bearings working in hybrid mode show almost constant damping performance throughout the range of radial load (\bar{W}_r). When bearing semi cone angle is increased from $\gamma = 5^\circ$ to 30°, the damping coefficient (\bar{C}_{22}) is also increased for hybrid and hydrostatic mode of bearing operation. Further, it has been investigated that the performances of hole-entry bearings in hydrostatic mode are superior to the hole-entry bearings in hybrid mode. However, semi cone angle $\gamma=30^\circ$ bearing indicates the higher damping performance in hydrostatic mode among the other bearings. Hence, the conical bearing adjusted for constant flow valve restriction may be suggested for their enhance characteristics in hydrostatic case than hybrid case. When the conical bearing is operating in hybrid mode at (\bar{W}_r) = 2.0, the percentage change in (\bar{C}_{22}) with reference to base bearing angle $\gamma = 5^\circ$, is noted of the order of 10.51 %, 44.41 % and 110.54 % for $\gamma = 10^\circ, 20^\circ$ and 30° semi cone angles respectively. Likewise, the percentage change in (\bar{C}_{22}) for conical journal bearing operating in hydrostatic mode with reference to hybrid mode, is noted of the order of 30.35 %, 27.77 %, 24.93 % and 23.84 % for bearings with $\gamma = 5^\circ, 10^\circ, 20^\circ$ and 30° respectively.

Threshold speed ($\bar{\omega}_{th}$) versus load in radial direction (\bar{W}_r)

Figure 12 indicates the plot of threshold speed ($\bar{\omega}_{th}$) of journal for varying radial load (\bar{W}_r) in hybrid mode for bearings with $\gamma = 5^\circ, 10^\circ, 20^\circ$ and 30° . It has been observed that when the load (\bar{W}_r) in radial direction is increased, journal threshold speed $\bar{\omega}_{th}$ is decreased. However, bearing cone angle $\gamma = 30^\circ$ depicts higher threshold speed among the other bearings. The higher threshold speed $\bar{\omega}_{th}$ could be achieved when the conical bearings are operated at lower loadings. When the hole-entry conical bearing is made to operate in hybrid mode at (\bar{W}_r) =2.0, the change in percentage of ($\bar{\omega}_{th}$) with respect to 5° base bearing operating in hybrid mode, is observed of the order of 1.71 %, 2.7 % and 1.18 % for bearing angles $\gamma = 10^\circ, 20^\circ$ and 30° respectively.

Conclusions

Conical journal bearing systems with hole-entry, adjusted for constant flow valve in hybrid and hydrostatic mode have been studied using FEM. The present study also encompassed the bearing performance for varying semi cone angles. With regards to the results found from the numerical method, the following conclusions are made:

- Maximum pressure (\bar{p}_{max}) is significantly increased for conical bearing with hole-entry operating in hydrostatic mode corresponding to hybrid mode.
- Bearing fluid film thickness is sufficiently higher when operating in hybrid mode for $\gamma = 5^\circ$ and 10° bearings. The bearing flow (\bar{Q}) is observed to be constant through the bearing operation.
- Stiffness coefficient (\bar{S}_{11} and \bar{S}_{22}) show significant enhancement in hydrostatic mode for bearing semi cone angle $\gamma = 30^\circ$ to that of other semi cone angles.
- Direct damping coefficients (\bar{C}_{11}) of conical journal bearings with hole-entry, are almost close when operating in hydrostatic and hybrid mode. However, significant damping (\bar{C}_{22}) is noticed in hydrostatic mode for increase in radial loading (\bar{W}_r)
- Journal threshold speed ($\bar{\omega}_{th}$) is found decreasing for radially loaded conditions for different conical bearings with hole entry operating in hybrid mode.

Compliance with ethical standards

Conflict of interest: The authors declare that they have no conflict of interest.

References

- [1] K.J. Stout, W.B. Rowe, Externally pressurized bearings-design for manufacturer, Part 1-Journal bearing selection, *Tribology International*, 7(3)(1974), pp.98-106. [https://doi.org/10.1016/0041-2678\(74\)90009-8](https://doi.org/10.1016/0041-2678(74)90009-8)
- [2] K.J. Stout, W.B. Rowe, Externally pressurized bearings design for manufacturer, Part 3-Design of liquid externally pressurized bearings for manufacture including tolerancing procedures, *Tribology International*, 7(5) (1974), pp.195-212. [https://doi.org/10.1016/0041-2678\(74\)90118-3](https://doi.org/10.1016/0041-2678(74)90118-3)
- [3] T.J. Prabhu, N. Ganesan, Characteristics of conical

- hydrostatic thrust bearings under rotation, *Wear*, 73(1) (1981), pp.95-122. [https://doi.org/10.1016/0043-1648\(81\)90213-1](https://doi.org/10.1016/0043-1648(81)90213-1)
- [4] T.J. Prabhu, N. Ganesan, Analysis of multi-recess conical hydrostatic thrust bearing under rotation, *Wear*, 89(1) (1983), pp.29-40. [https://doi.org/10.1016/0043-1648\(83\)90212-0](https://doi.org/10.1016/0043-1648(83)90212-0)
- [5] Z. Nowak, K. Wierzcholski, Flow of a Non-Newtonian power law lubricant through the conical bearing gap. *Acta Mechanica*, 50(1984), pp.221-230. <https://doi.org/10.1007/BF01170962>
- [6] M.F. Khalil, S.Z. Kassab, A.S. Ismail, Performance of externally pressurized conical thrust bearing under laminar and turbulent flow conditions, *Wear*, 166(2) (1993), pp.147-154. [https://doi.org/10.1016/0043-1648\(93\)90256-L](https://doi.org/10.1016/0043-1648(93)90256-L)
- [7] S. Yoshimoto, T. Kume, T. Shitara, Axial load capacity of water lubricated hydrostatic conical bearings with spiral grooves for high speed spindles: Comparison between rigid and compliant surface bearings, *Tribology International*, 31(6) (1998), pp.331-338. [https://doi.org/10.1016/S0301-679X\(98\)00043-7](https://doi.org/10.1016/S0301-679X(98)00043-7)
- [8] S. Yoshimoto, S. Oshima, S. Danbara, T. Shitara, Stability of water-lubricated, hydrostatic conical bearings with spiral grooves for high-speed spindles, *ASME Journal of Tribology*, 124(2) (2002), pp.398-405. <https://doi.org/10.1115/1.1405815>
- [9] P. Sinha, P. Chandra, S.S. Bhartiya Thermal effects in externally pressurized porous conical bearings with variable viscosity, *Acta Mechanica*, 149(2001), pp.215-227. <https://doi.org/10.1007/BF01261673>
- [10] R.B. Ingle, B.B. Ahuja, An experimental investigation on dynamic analysis of high speed carbon-epoxy shaft in aerostatic conical journal bearings, *Composites Science and Technology*, 66(3-4) (2006), pp.604-612. <https://doi.org/10.1016/j.compscitech.2005.03.021>
- [11] H. Guo, X.M. Lai, S.Q. Cen, Theoretical and experimental study on dynamic coefficients and stability for a hydrostatic/ hydrodynamic conical bearing, *ASME Journal of Tribology*, 131(4) (2009), pp.041701-041707. <https://doi.org/10.1115/1.3176991>
- [12] S.C. Sharma, V.M. Phalle, S.C. Jain, Performance analysis of a multi-recess capillary compensated conical hydrostatic journal bearing, *Tribology International*, 44(5) (2011), pp.617-626. <https://doi.org/10.1016/j.triboint.2010.12.012>
- [13] S.C. Sharma, V.M. Phalle, S.C. Jain, Influence of wear on the performance of a multi-recess conical hybrid journal bearing compensated with orifice restrictor, *Tribology International*, 44(12) (2011), pp.1754-1764. <https://doi.org/10.1016/j.triboint.2011.06.032>
- [14] S.C. Sharma, A.K. Rajput, Influence of micropolar lubrication on the performance of 4-pocket capillary compensated conical hybrid journal bearing, *Advances in Tribology*, Article ID 898252 (2012), pp.1-18. <http://dx.doi.org/10.1155/2012/898252>
- [15] A.Y. Korneev, Static characteristics of conical hydrodynamic bearings lubricated by turbine oil, *Russian Engineering Research*, 32(2012), pp. 251-255. <https://doi.org/10.3103/S1068798X12030148>
- [16] A.Y. Korneev, Influence of turbulence on the static characteristics of conical journal bearings, *Russian Engineering Research*, 32(4) (2012), pp.338-342. <https://doi.org/10.3103/S1068798X12040156>
- [17] A.Y. Korneev, Rigid rotor dynamics of conical hydrodynamic bearings, *Russian Engineering Research*, 34(3) (2014), pp.131-135. <https://doi.org/10.3103/S1068798X14030083>
- [18] A.K. Rajput, S.C. Sharma, Analysis of externally pressurized multi-recess conical hybrid journal bearing system using micropolar lubricant, *Proceedings of IMechE, Part J: Journal of Engineering Tribology*, 227(9) (2013), pp.943-961. <https://doi.org/10.1177/1350650112469272>
- [19] N.K. Rana, S.S. Gautam, S.Verma, Static characteristics of conical hydrostatic journal bearing under micropolar lubrication, *Journal of Institution of Engineers India Series C*, 95(4) (2014), pp.375-381. <https://doi.org/10.1007/s40032-014-0148-7>
- [20] A.K. Rajput, S.C. Sharma, Stability of a constant flow valve compensated multi-recess conical hybrid journal bearing operating with micropolar lubricant, *Lubrication Science*, 26(5) (2014), pp.347-362. <https://doi.org/10.1002/lis.1264>
- [21] N.K. Rana, S.S. Gautam, S.Verma, Performances of 6-pocket compensated conical hydrostatic journal bearing under micropolar lubrication. *Proceedings of the World Congress on Engineering and Computer Science*. San Francisco, USA. October 21-23, 1(2015).
- [22] N.K. Rana, S.S. Gautam, S.Verma, Performance characteristics of constant flow valve compensated conical multirecess hybrid journal bearing under micropolar lubrication, *International Journal of Design Engineering*, 6(3) (2016), pp.218-236. <https://doi.org/10.1504/IJDE.2016.079030>
- [23] N.K. Rana, S.S. Gautam, S.Verma, Comparative study on the effect of recess on conical hybrid journal bearing compensated with CFV under micropolar fluid lubrication, *Tribology Online*, 11(3) (2016), pp.474-486. <https://doi.org/10.2474/trol.11.474>
- [24] P.G. Khakse, V.M. Phalle, S.S. Mantha, Performance analysis of a non-recessed hybrid conical journal bearing compensated with capillary restrictors. *ASME Journal of Tribology*, 138(1) (2016), pp.0117031-9. <https://doi.org/10.1115/1.4030808>
- [25] P.G. Khakse, V.M. Phalle, S.S. Mantha, Orifice compensated performance characteristics of hybrid hole-entry conical journal bearing, *Proceedings of IMechE, Part J: Journal of Engineering Tribology*, 231(3) (2017), pp.316-331. <https://doi.org/10.1177/1350650116654803>
- [26] R. Sinhasan, S.C. Sharma, S.C. Jain, Performance characteristics of a constant flow valve compensated multi-recess flexible hydrostatic journal bearing, *Wear*, 134(2) (1989), pp.335-356. [https://doi.org/10.1016/0043-1648\(89\)90135-X](https://doi.org/10.1016/0043-1648(89)90135-X)